Wear xxx (xxxx) xxx

Contents lists available at ScienceDirect

Wear

journal homepage: www.elsevier.com/locate/wear

Tribological behaviour of a graphite–phenolic resin solid lubricant under high mechanical load

Omar Zouina [a,*], Alexandros Lappas [a], Martin Dienwiebel [a,b]

[a] Karlsruhe Institute of Technology (KIT), Institute for Applied Materials (IAM), MicroTribology Center μTC, Strasse am Forum 7, 76131 Karlsruhe, Germany
[b] Fraunhofer-Institute for Mechanics of Materials IWM, MicroTribology Center μTC, Woehlerstrasse 9, 79108 Freiburg, Germany

ARTICLE INFO

Dataset link: https://doi.org/10.35097/hw4299hh47qytpg6

Keywords:
Solid lubricant
Graphite
Phenolic resin
Coating
Third body
Sliding wear

ABSTRACT

Graphite can be considered as a suitable solid lubricant in highly loaded contacts and extreme environmental conditions, where conventional liquid lubricants or greases are of restricted use (e.g. in rolling bearings). Indeed, graphite as a solid lubricant, has been reported to exhibit good lubricating properties even at high mechanical loads quite well, though it yielded a limited lifetime. The use of binders, (i.e. resins) stems in a continuance of the adequate lubricating behaviour, as well as, an improved wear resistance. This work aims to understand the friction and wear behaviour of solid lubricating coatings consisting of a graphite–phenolic resin blend. For this investigation various coatings, with three different graphite contents, applied using the simple airspray method on 100Cr6 bearing steel plates of comparable thicknesses were examined. When tested on a ball-on-flat reciprocating motion, we find that compared to pure graphite coatings, the lifetime indeed is significantly enhanced reaching up to 10 000 cycles, whilst keeping a coefficient of friction around 0.1. During the experiments with the higher graphite content specimen a transfer layer on the counterbody was observed as well as a thin compressed layer of material. Raman spectroscopy reveals that the observed carbonaceous tribofilm consists of what could be a rather amorphous graphite-like material which is responsible for the favourable lubricity.

1. Introduction

Lubricants are used in the majority of employed mechanical systems to mitigate their contacts, thus, reducing friction and wear. Solid lubricants, in particular, have been of interest to many tribologists for their stability and favourable tribological properties in harsh functioning conditions, e.g. high temperatures, loads or in vacuum, where conventional liquid or grease lubrication can be of seldom use [1,2]. Graphite is notably one of the first used solid lubricants in technical applications. It can be found in high-temperature grinding [3], in rail systems [4] and in cryogenic conditions as well [5]. Graphite can as well be incorporated within sliding bearings alongside metals or alloys, for instance bronze, but in such application the loads are rather low [6]. The use of graphite in highly loaded applications such as rolling bearings remains quite limited.

Ever since the unveiling of its lamellar structure and by Bragg in 1928 [7]. Graphite has been thoroughly, especially at smaller scales, investigated by numerous researchers using experimental and simulation methods [8,9]. At the nanoscale it has been reported to exhibit superlubricity, a very low Coefficient of Friction (CoF) of 0.001, due to the incommensurability of contact between the lattices [10] and the contribution of atoms situated at the edges (pinning sites) [11]. Achieving superlubricity on a larger scale was proven to be a challenge, since on such scales the presence graphite on both sides of the interface between tribopairs is not obvious, this implicates the necessity of the formation of a transfer film [12].

On larger scales, graphite tends to exhibit typically a friction coefficient between 0.08 and 0.2 in ambient air and around 0.8 in vacuum. Such distinct frictional behaviour is well established in the literature. In fact graphite has been proven to show a poor tribological behaviour in vacuum due to dusting effect, thus, yielding higher friction and wear than in ambient atmosphere [13,14]. The humidity dependency of graphite lubrication was supported by experiments and simulations [15,16]. The aforementioned environmental influenced was demonstrated by Marchetto et al. to be due to surface passivation resulting in low shear strength and adhesion [17]. Furthermore at higher loads, Morstein et al. reported, by means of experiments and simulations, that at higher loads the presence of humidity triggers a structural transition towards turbostratic carbon when graphite is used as a solid lubricant, this finding has filled a gap in the understanding of the mechanism lying under graphite lubrication [15].

* Corresponding author.
E-mail addresses: omar.zouina@kit.edu (O. Zouina), martin.dienwiebel@kit.edu (M. Dienwiebel).

https://doi.org/10.1016/j.wear.2025.205936
Received 20 September 2024; Received in revised form 20 January 2025; Accepted 3 February 2025
Available online 23 February 2025

Table 1
Coating thicknesses.

Percentage	Thickness
10Gr	7, 17, 21 μm
20Gr	7, 16.1, 21.6 μm
30Gr	7, 17, 23.2 μm

Aside from the influence of the surrounding environment, several factors could affect the tribological behaviour of graphite, and its 2D allotrope graphene. Several studies took interest in the impact of the physical properties of the lubricant, its thickness or the substrate's influence. Li et al. demonstrated using friction force microscopy and FEM simulations that the thickness of the lubricant impacts friction when there is a weaker adhesion between the substrate and the lubricant [18]. Morstein et al. reported that air sprayed graphite coatings can lubricate highly loaded contacts quite well. It was shown that a lower thickness resulted in lower friction but a more severe wear; on the other hand, a higher thickness had the opposite effect. Moreover, they highlighted that the usage of a rougher substrate resulted in a more benign tribological performance [19]. Similarly, recent work conducted by Abe et al. investigated the impact of the morphology and thickness of airspray coatings on their tribological properties and reported that the friction and wear of such coatings is mainly influenced by their thickness. They also linked the higher coating porosity to higher wear [20]. Such reported findings demonstrate that using rather facile coating application techniques can result in favourable tribological properties. Yet, there is still room for improvement in terms of wear resistance.

In the quest of extending the lifetime of the advantageous lubricating properties of graphite, binders were mixed with graphite by several researchers. Phosphate-based materials were reported in the literature to exhibit a stable and low CoF at elevated temperatures, however the yielded wear rates were quite subsequent [21,22]. Different authors reported that the use of phenolic resin as a binder results in low friction and wear at a wide range of temperatures. As well as a successful transfer of graphite to the counter surface confirmed with a Raman analysis of the opposing tribosurfaces after the tribological test, thus, ensuring a long-term lubrication [23–26]. Xu et al. have reported that combining laser surface texturing with the use of graphite–phenolic resin system can further reduce friction meanwhile ensuring graphite transfer film to the counter surface in dry conditions [27]. Zheng et al. have reported that such solid lubricants have superior tribological properties at room temperature than at cryogenic conditions [28].

In this work, we investigate the friction and wear of air sprayed graphite–phenolic resin coatings. Different coatings with various thicknesses and graphite ratios were tested using a microtribometer. To assess the lifetime of these coatings, the studied samples were tested for different number of cycles. Afterwards, techniques such as confocal microscopy, while-light interferometry, scanning electron microscopy, and Raman spectroscopy were used to describe qualitatively and quantitatively the wear behaviour of such coatings. Based on previous results, our hypothesis is that the graphite content should strongly affect friction and wear mechanisms in order to examine the usability of such solid lubricants for rolling bearing applications.

2. Materials and methods

2.1. Sample preparation

100Cr6 rolling bearing steel rings (INA rolling bearings, Schaeffler, Germany) were cut into $17 \times 6 \times 7$ mm plates and served as base bodies for the tribological experiments. The bearings plates were kept in their original surface state and their measured average roughness was $S_A = 0.178 \pm 0.019$ μm. The samples were ultrasonically cleaned for 15 min using acetone followed by isopropanol. Lastly they were dried using pressurized air to avoid corrosion. The same cleaning protocol was adopted for the 100Cr6 steel spheres which were used as counterbodies for the tribological tests.

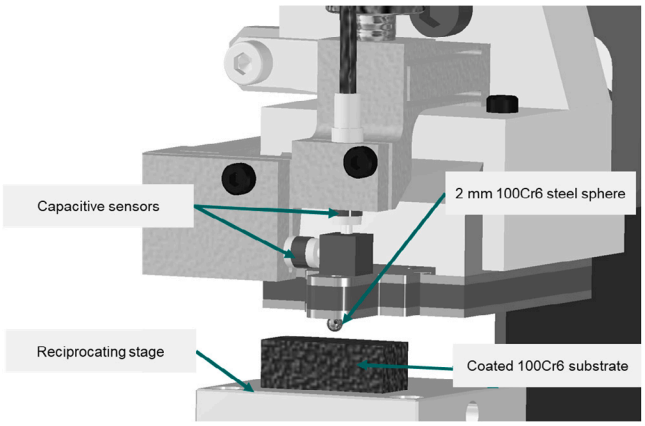

Fig. 1. Schematic representation of the microtribometer.

A graphite–phenolic resin blend suspension (Everlube 629, Everlube Products, USA) was diluted in methyl ethyl ketone MEK (≥99% purity, VWR international, USA) in a ratio of 1:3 respectively. In order to study the impact of different graphite contents on the tribological behaviour, additional synthetic graphite powder (APS 7-11 μm purity 99%, Thermo scientific, USA) was added into the mixture. The aforementioned graphite powder was added to the diluted suspension at various volume fractions and these suspensions were then ultrasonically mixed for an hour. Note that the suspension marked as "0Gr" corresponds to the original suspension delivered from the company (in which the existence of graphite was stated); hence, the percentages reported afterwards refer to the additional amount of graphite.

For the solid lubricant coating application onto the bearing steel plates, the prepared suspensions were applied using an airbrush spray gun (Harder & Steenbeck Ultra, Harder & Steenbeck GmbH & Co.KG, Germany). The spraying process was conducted manually at a working distance of about 15 cm. The steel specimens were covered with the prepared suspensions by performing multiple sweeps across, this allowed the preparation of a large range of coating thicknesses. The coated specimens were subjected to a curing heat treatment of the graphite–phenolic resin at 150±15 °C. Following the curing process, the coating thickness was determined for all coated specimens. Therefore, one end of the bare steel plates was covered by a heat-resistant polyimide tape with silicon-based adhesive (Scotch 5413, 3M, USA). Thus, after removing the tape, an interface between the coated and uncoated parts allowed to determine the step height (i.e. the coating thickness) using confocal microscopy. Specifications of the tested coating thicknesses are given as in Table 1. For simplification reasons, we refer to these thicknesses as 7, 17 and 21 μm.

2.2. Tribological testing

A home-made ball-on-flat microtribometer was used for the tribological investigation of the coated steel plates in linear reciprocating sliding. The microtribometer, as shown in Fig. 1, uses a set of two capacitive sensors (Micro-epsilon GmbH, Germany) placed in the normal and tangential directions and two mounted step-motorized stages ensuring motion in the z-direction and x-direction (Attocube Systems AG, Germany). 2 mm 100Cr6 steel spheres (Grade 10, TIS GmBH, Germany) were used as counterbodies. Each counterbody was glued with cyanoacrylate glue (Pattex liquid superglue, Henkel AG & Co. KGaA, Australia) onto two different self-built double-leaf cantilevers with spring constants of $k_t = 5.034$; $k_N = 2.786$ mN/μm and $k_t = 5.768$; $k_N = 1.965$ mN/μm respectively. No residual glue was in the contact

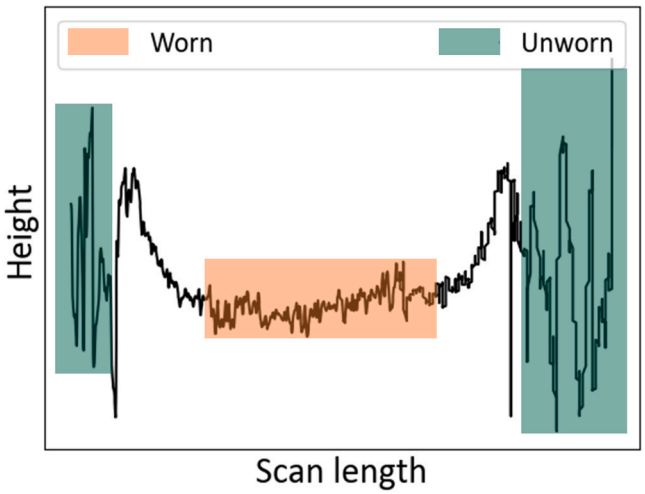

Fig. 2. Representation of the wear depth measurement method from a surface profile.

area since the spheres were cleaned before the tribological test. It should be noted that for each experiment, a different batch of materials was used, on different days. Moreover, three repeats were made to guarantee that our results were repeatable, except for the 10 000 cycles tests, each tests was repeated twice at least given the length of each test. All experiments were conducted at around ≈30°C and a relative humidity between 20 and 40% RH.

Different thicknesses of the graphite–phenolic resin coatings (as detailed in Table 1) were tested at a normal force of $F_N = 402$ mN resulting in a maximum Hertzian contact pressure of around 1 GPa. In order to assess the wear behaviour (i.e. the lifetime) of these coatings, the specimens were tested for 500, 1000 and 10 000 cycles; at a sliding distance of 1 mm and sliding speed of 0.5 mm.s^{-1}. The normal and lateral forces were constantly measured throughout the tribological test. The same experiment was conducted on bare uncoated steel as a reference.

2.3. Surface characterization

Prior to and after all tribological experiments, confocal microscopy (Sensofar Plμ, Sensofar, Spain) and white-light interferometry (Bruker Contour GT-K 3D optical profiler, Bruker, USA) were used to examine wear scars and counterbodies, as well as the topography of the uncoated specimens. The obtained topographs were then analysed using SensoMap (a surface analysis software based on Digitalsurf's Montainsmap), to obtain roughness parameters and to conduct further wear scar analyses.The same software was used to determine the wear depths, as shown in Fig. 2, by analysing at least three distinct profiles that ranged through unworn and worn regions of the wear track to ensure reproducibility and accuracy.

A further, qualitative, analysis of the surfaces was conducted using a dual beam scanning electron microscope focused ion beam (Helios NanoLab DualBeam 650, ThermoFischer Scientific, USA). A Platinum protective layer (≈1 μm) was deposited on the area of interest before the ion beam cutting. Cross sections of 30 μm in length and ≈10 μm in width were performed with the Ga FIB. The obtained cross section were

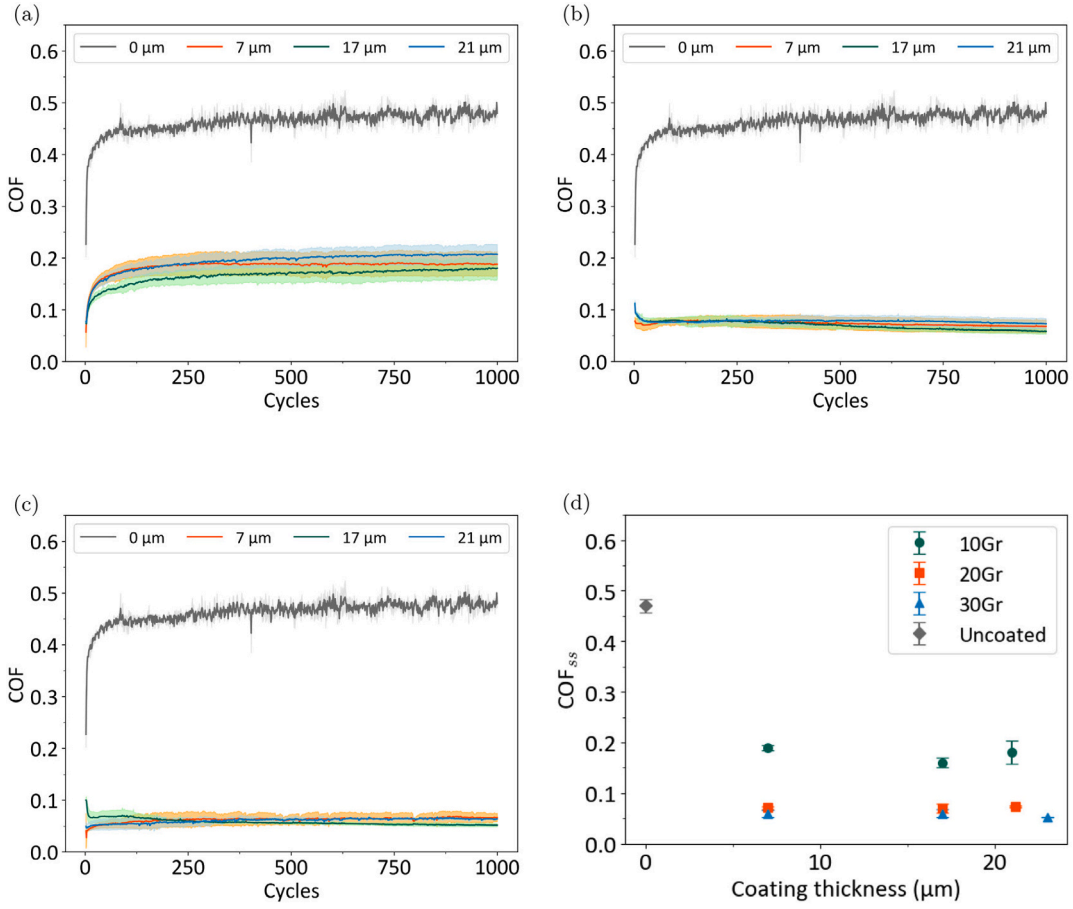

Fig. 3. Coefficient of friction of coated 100Cr6 bearing steel specimens versus a 100Cr6 sphere at different graphite–phenolic resin coatings thicknesses and graphite contents. (a) CoF of 10% added graphite (10Gr), (b) CoF of 20% (20Gr), (c) CoF of 30% (30Gr), (d) average CoF at the steady state (COF_{ss}) of the overall tested thicknesses and added graphite contents.

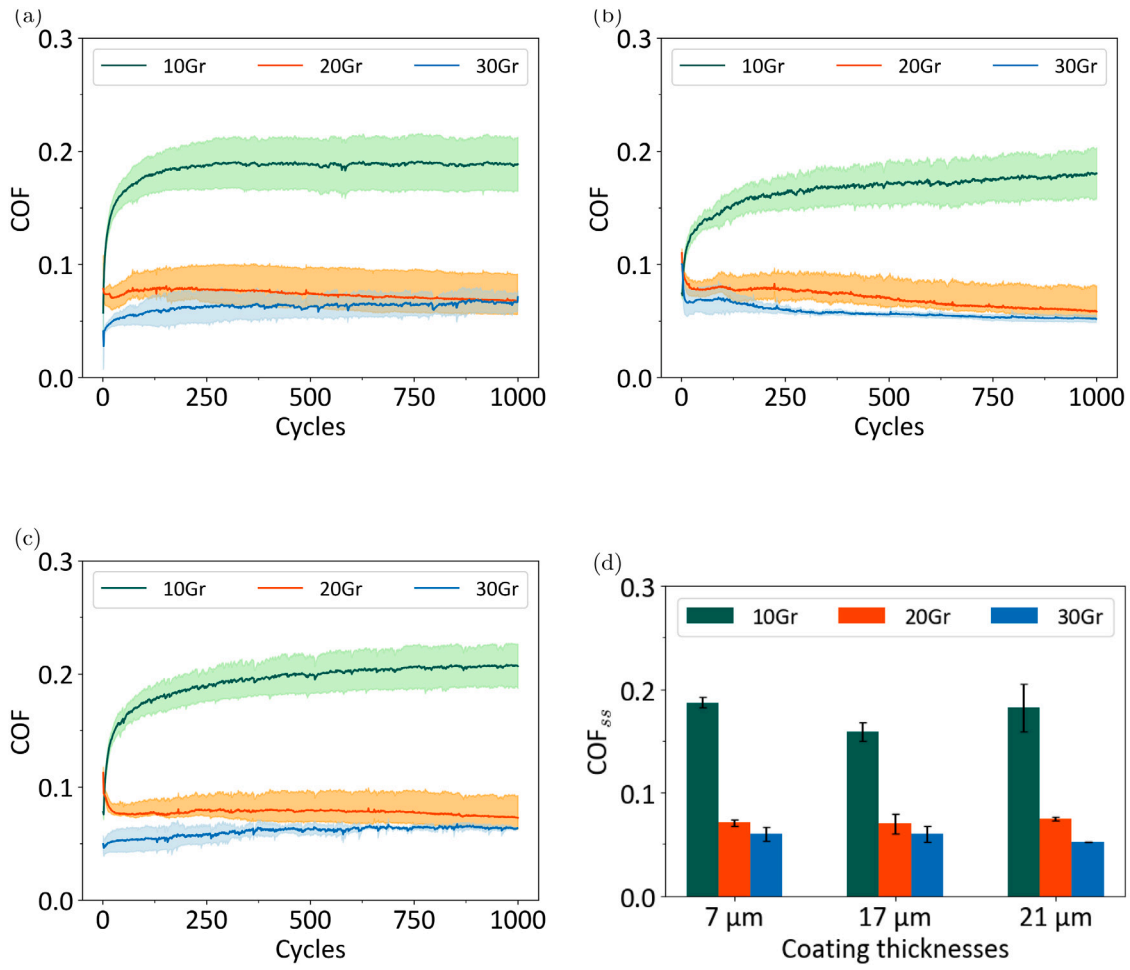

Fig. 4. Coefficient of friction of coated 100Cr6 bearing steel specimens versus a 100Cr6 sphere at different graphite–phenolic resin coatings of different graphite contents. (a) CoF at 7 µm, (b) CoF at 17 µm, (c) CoF at 21 µm, (d) average CoF at the steady state ($COFss$) of the overall tested thicknesses and added graphite contents.

examined using a scanning eletron microscope in secondary electrons (SE) mode at an accelerating voltage of 2 kV and current of 0.8 nA. Raman measurements of the unworn coatings and wear scars were performed using a 532 nm pico-Raman spectrometer (PicoRaman M3, Timegate Instruments, Finland) equipped with a 20x microscope objective lens (Leica microsystems GmbH, Germany) with the laser power set at 2.5 mW to avoid any beam-induced damage to the samples.

3. Results

3.1. Friction

Fig. 3 shows the evolution of the friction coefficient over the number of cycles. Each curve represents the average CoF value of multiple tests (as mentioned in Section 2), the shaded areas around each curve represent the standard deviation. In Fig. 3(a) the CoF evolution the different thicknesses of the 10Gr specimens is represented. It can be seen that all coating thicknesses exhibit a quite similar trend. Similarly in Fig. 3(b) and 3(c), similar trends are observed, with lower CoF values and overall a shorter running-in period with the 20Gr and 30Gr respectively. Thus, it can deduced that the coating thickness has no direct impact on the frictional behaviour of such solid lubricating coatings. Furthermore, in Fig. 3(d) we show the mean steady-state coefficient of friction values over 1000 cycles. The obtained results confirm the lack of a direct correlation between the coating thickness and the coefficient of friction, meanwhile the graphite content remains more affecting (i.e. lower CoF values are recorded with higher graphite contents).

To highlight the aforementioned trend further. Fig. 4 shows the evolution of the friction coefficient over the number of cycles of the different graphite contents. Fig. 4(a) shows the CoF evolution of the different graphite contents at a coating thickness of 7 µm, It can be seen clearly that the higher graphite content brings better lubricity. In addition, Fig. 4(b) and 4(c) exhibit a congruent trend, with the 30Gr coatings showing the most potent lubricity. Fig. 4(d) summarizes the shown trend, the average steady-state friction coefficient values over 1000 cycles demonstrate that the 10Gr recorded the highest CoF values and a slight difference is observed between the 20Gr and 30Gr. This verifies the previously shown results.

In order to assess the lifetime of the studied coatings, longer tribological tests were performed. Each specimen was tested for 10 000 cycles at least twice to ensure repeatability of the obtained results. Fig. 5 shows the evolution of the friction coefficient over the larger number of cycles (i.e. 10 000 cycles) of the different graphite contents. Fig. 5(a) shows the CoF evolution of the different graphite contents at a coating thickness of 7 µm, Fig. 5(b) and 5(c) represent the evolution of the friction coefficient over the number of cycles at coating thicknesses of 17 µm and 21 µm respectively. Overall, the trend observed in the

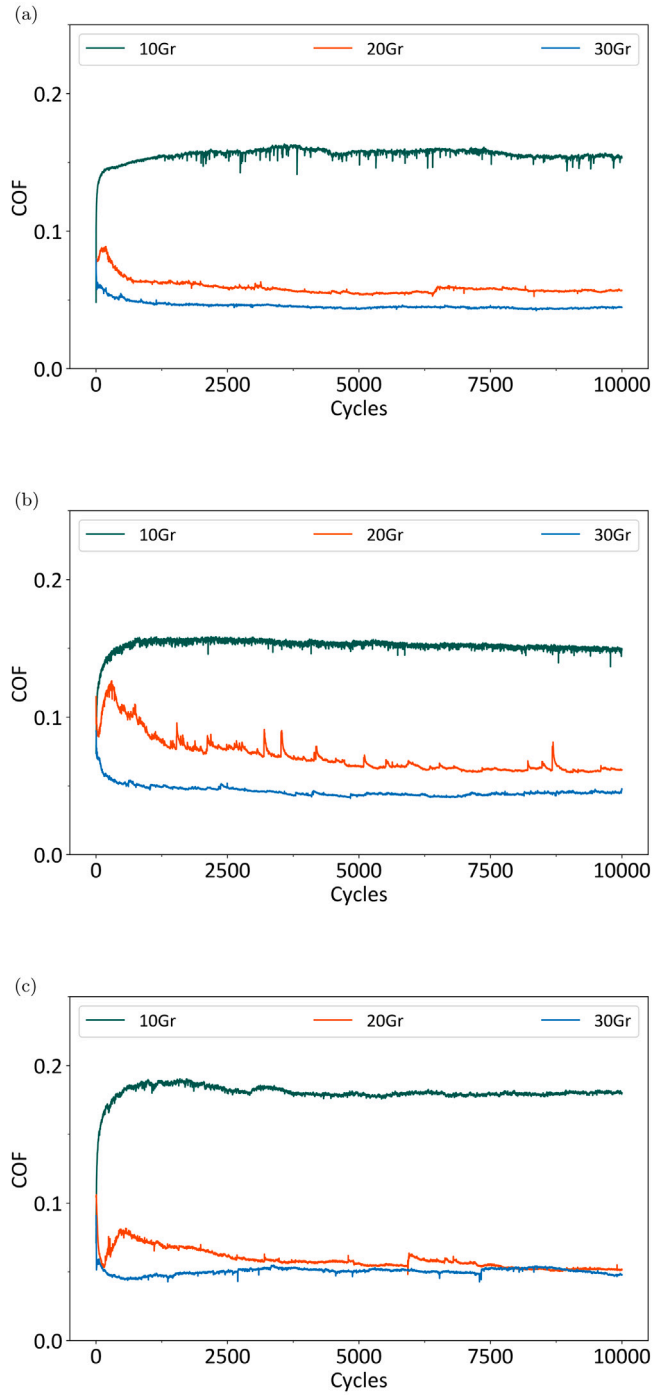

Fig. 5. Coefficient of friction of coated 100Cr6 bearing steel specimens versus a 100Cr6 sphere at different graphite–phenolic resin coatings of different graphite contents after 10 000 cycles. (a) CoF at 7 µm, (b) CoF at 17 µm, (c) CoF at 21 µm.

shorter tests is conserved, with the higher graphite content specimens exhibiting the lowest CoF values without lowering the lifetime within the tested period.

3.2. Wear

Fig. 6 displays an overview of the observed wear behaviour of the moving tribopairs (i.e. different coatings with various graphite contents and their respective counterbodies). Fig. 6a shows that with the lower graphite content the main present phenomenon is a visible compression of the coating and a more discernible wear of the counterbody. On the other hand, Fig. 6 shows that with the 20Gr coating, we can observe a rather small area of compression at the edge of the wear scar, and the formation of a tribofilm in the middle. In addition, the 30Gr specimens exhibit a different trend with no apparent compression of the coating, an overall deeper wear scar and tribofilm formation within the wear track, We can also see from Fig. 6b and c, that a higher graphite content promotes forming a transfer film on the counter surfaces.

The average wear depths of the different coatings and their corresponding counterbodies are shown in Fig. 7. After a tribological test of 500 cycles we can observe in Fig. 7(a) that with a lower graphite content, the wear is yielded more in the counterbody than in the coating. On the other hand with the 20Gr and 30Gr coatings, we observe a tendency of wearing off the graphite–phenolic resin coating more than the counterbody. Similarly after 1000 cycles, we observed overall the same trend in Fig. 7(b). Furthermore, we can observe that when a higher graphite content (20Gr and 30Gr) is used, the wear depth obtained with the higher coating thicknesses does not increase more than the recorded values after 500 cycles. Fig. 7(c) shows the average wear depths of the different coatings and their corresponding counterbodies after a tribological test of 10 000 cycles. The findings corroborate what was found in the shorter tests. With higher graphite contents, the wear is yielded more in the solid lubricant coating than in the steel sphere. However, similarly to the shorter tribological tests, with the 10Gr specimens the observed wear was mainly conceded by the counter surface.

3.3. Surface characterization

Fig. 8 shows the Scanning Electron Microscopy (SEM) images of the wear tracks of different graphite contents, and their respective cross sections obtained with FIB, after the tribological test. It is shown on Fig. 8a that the dominant phenomenon after the tribological test is coating compression, when a lower graphite content (i.e. 10Gr) is used. On the other hand, as shown in Fig. 8b and c, with a higher graphite content, a different phenomenon is perceived. At such graphite contents, coating delamination and tribofilm formation are promoted. We also note that with the 20Gr coatings, a coating compression area is perceived at the edge of the wear scar (Fig. 8b). The FIB cross section images, as shown in Fig. 8d, e an f, validate the aforementioned phenomena.

In order to further enrich our understanding of the undergoing phenomena with such coatings, we performed a Raman analysis on the unworn coatings as well as post-tribological tests at different cycle numbers, the results are displayed in Fig. 9. Fig. 9(a) shows that for the unworn coatings no clear graphitic peaks can be seen, except for the 30Gr samples where a D-band is rather depictable. The Raman spectrum of the 20Gr sample has a similar aspect with the presence of a less intense D-band. On the other hand, the lower graphite containing coating shows none of the characteristic peaks seen with graphitic structures. The Raman spectra of the higher graphite contents (i.e. 20Gr and 30Gr) exhibit more graphitic peaks after the tribological tests (as shown in Fig. 9(b), 9(c) and 9(d)). However, the presence of a different chemistry can be perceived that in the 10Gr coatings spectra.

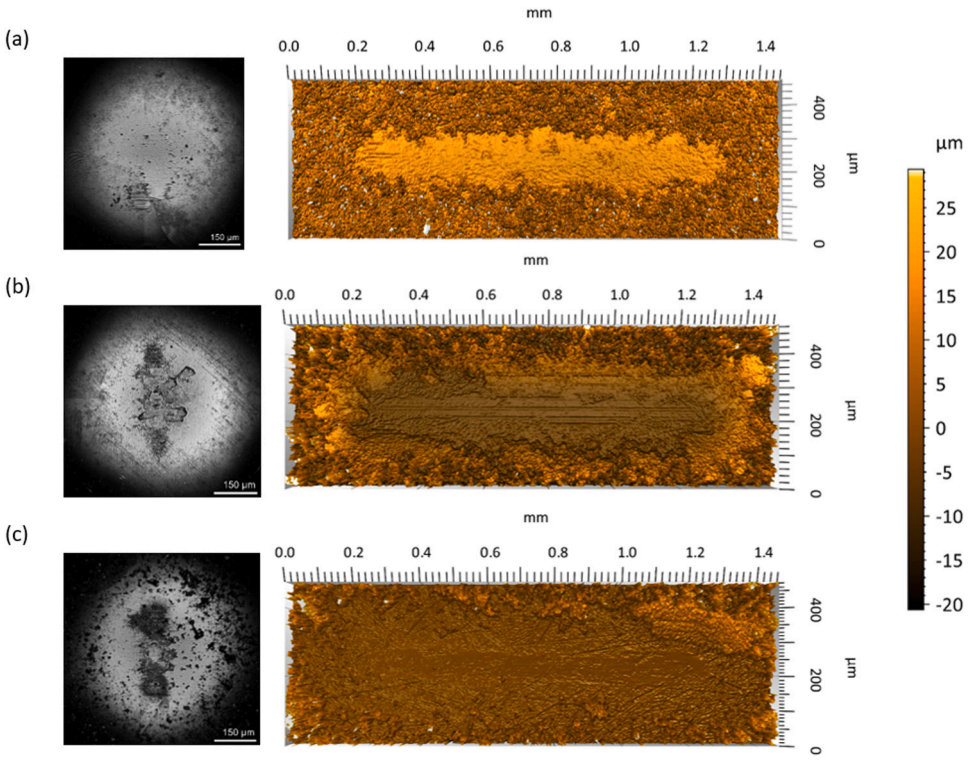

Fig. 6. Confocal microscopy image of the 100Cr6 steel counterbodies after the tribological test (left), top view 3D representation of the wear tracks and average coloured height scale bar (right). (a) 10Gr, (b) 10Gr, (c) 30Gr.

4. Discussion

4.1. Friction and wear

The experimental results reported in this paper clearly demonstrate that, unlike previous results on pure graphite, with such coatings no thickness dependence could be seen. Indeed, with different graphite contents, similar evolutions of the friction coefficient were shown in Fig. 3. In fact, a different trend is observed when pure graphite is used, since with a higher coating thickness a higher friction is yielded [19]. On the contrary, the graphite content seems to have a stronger impact on the frictional behaviour, as shown in Fig. 4, a lower graphite content (i.e. 10Gr) is evidently linked to a higher CoF value throughout the tested thicknesses with an optimum low friction coefficient recorded with the 30Gr specimens. This finding is in agreement with the work reported in [26]. Moreover, the evidence presented in Fig. 5 clearly demonstrate that graphite–phenolic resin coating can lubricate a highly loaded contact for an extended period of time (i.e. 10 000 cycles).

As for the yielded wear behaviour, we observed two main distinct wear modes. With the lower graphite content (10Gr), the wear is mostly concentrated in the counter surface (shown in Fig. 6a and Fig. 7), this is due to the absence of a transfer film on the 100Cr6 steel sphere after the tribological test. In addition, more precisely on the coating side only compaction is observed within the wear scar, this is clearly shown on Fig. 6a and 8a. In contrast, when 20% of additional graphite to the coating (20Gr coating) is used, a different phenomenon is perceived. Lower wear of the counterbody is seen, thanks to the apparent transfer film formed during the tribological test (as shown in Fig. 6b). In the SEM images of the wear track and the FIB cross section images in Fig. 8b, compression at the vicinity of the wear track is observed; within the wear some coating delamination as well as a tribofilm. Additionally, in this tribopair, most of the wear is concentrated in the coating since the formation of a transfer film is more promoted. Such findings are displayed in the average wear depth presented in Fig. 7. Moreover when more graphite is added (30Gr), we can perceive that a higher transfer to the counter surface is yielded (as shown in Fig. 6c). In addition, more coating delamination is seen and a more discernible tribofilm can be observed on the SEM images in Fig. 8c. We should also note that no coating compression was present at the wear track. Such wear behaviour is more similar to the one observed when pure graphite is used [19].

4.2. Raman analysis

The Raman analysis presented in Fig. 9 has provided us with further insights on the underlying tribochemical mechanisms during the tribological tests. In fact it can be depicted clearly that, with the higher graphite contents (20Gr and 30Gr), the apparition of graphitic peaks (i.e. D and G bands) as shown in Fig. 9(b), 9(c) and 9(d). Though, it should be noted that the observed D bands are more intense than their corresponding G bands, this finding provides evidence that the yielded tribofilm is not crystalline graphite. In fact, when graphite is analysed with Raman spectroscopy, the typical D bands exhibit lower intensities than the G bands [29]. Furthermore, under such high load and humidity range, a coating delamination coupled with a structural transition towards forming an amorphous turbostratic carbon tribofilm [15]. It could be stated that with the current results, that the wear mechanism with these coatings, when there is a sufficient graphite content in the contact, we could trigger a similar tribo-induced transition towards turbostratic carbon. Furthermore, we can see that the formed carbonaceous tribofilm stays quite stable even when subdued to longer tribological tests, since the observed peaks resist adequately (as shown in Fig. 9(d)). An observable reduction in the signal intensity of the 30Gr specimens which could be due to a reduction of the tribofilm thickness.

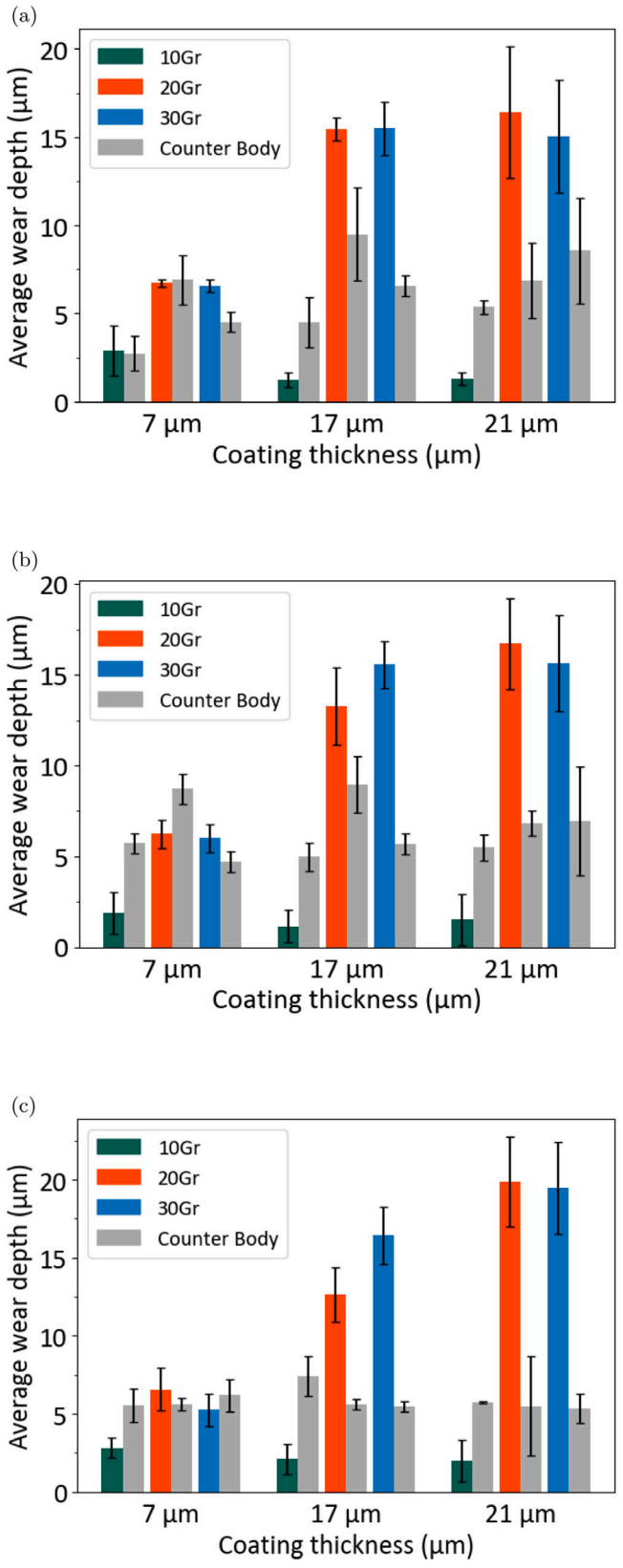

Fig. 7. Average wear depths in µm of the different coatings and their corresponding counterbodies after the tribological test. (a) after 500 cycles, (b) after 1000 cycles, (c) after 10 000 cycles.

In contrast when a lower graphite content is present in the coating, and under the same experimental conditions, no change in the Raman spectra was seen regardless of the number of sliding cycles (as shown in Fig. 9).

4.3. The wear mechanism

Based on the presented analyses, the wear mechanism of the studied airsprayed graphite–phenolic resin coatings can be describe depending on the graphite content as displayed in Fig. 10. When a lower graphite content is used, transfer layer formation on the counter surface is not favoured; the wear is subdued mainly by the counterbody with only a compression to be yielded by the coating. Furthermore higher graphite ratios seems to bear a contrasting mechanism. In fact, a reduced wear on the counter surface due to the formation of a transfer film, a yielded delamination of the coating and a tribofilm formation took place due to introducing more graphite flakes in the contact. Moreover a clear tribochemical transformation towards a more amorphous graphitic structure, potentially turbostratic carbon, seems to accordingly play a subsequent role in bearing a behaviour resembling that of pure graphite.

5. Conclusions

In this work, 100Cr6 bearing steel were coated using an airbrush gun with three different graphite–phenolic resin coatings with distinct graphite contents. After tribologically testing different thicknesses of such coatings in a highly loaded contact, a few conclusions can be derived:

- There is a significant improvement of the lifetime with the use of a graphite–phenolic resin blend compared to pure graphite, whilst keeping a comparable frictional behaviour.
- No coating thickness dependence was perceived, thus, the graphite content remains the prevailing parameter, with 30Gr exhibiting the lowest CoF values.
- With the lower graphite ratio, the counterbody takes the largest share of the wear, meanwhile when more graphite is present, transfer film formation are promoted.
- The tribo-induced chemical transition to a carbonaceous tribofilm, potentially turbostratic carbon, could explain the pure graphite-like wear behaviour observed in the tested specimens.

Declaration of competing interest

The authors declare that they have no known competing financial interests or personal relationships that could have appeared to influence the work reported in this paper.

The author is an Editorial Board Member/Editor-in-Chief/Associate Editor/Guest Editor for Wear and was not involved in the editorial review or the decision to publish this article.

Acknowledgements

This work is funded by the Deutsche Forschungsgemeinschaft (DFG). The project “Mechanism of Graphite Lubrication in Rolling Contact” (“Mechanismen der Graphitschmierung in Wälzkontakten”) is part of the priority program SPP2074 (grant number DI1494/7-2).

Data availability

The generated and processed datasets in this work are available on request from the authors through the KITOpen data repository under the DOI link: https://doi.org/10.35097/hw4299hh47qytpg6.

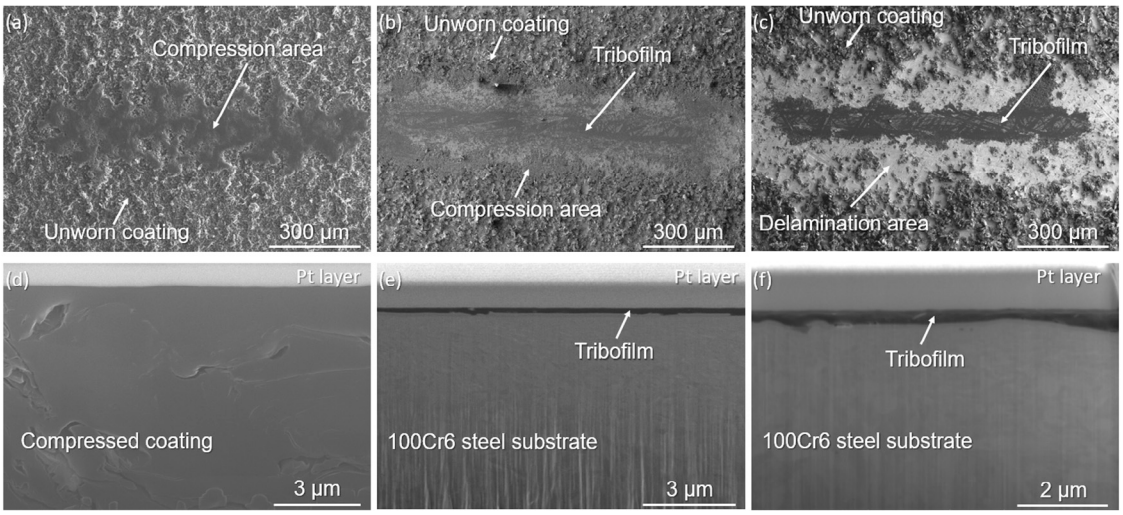

Fig. 8. Scanning Electron Microscopy (SEM) images of wear tracks and their respective cross sections taken after microtribometer experiments of different coatings containing distinct graphite contents. (a, d) 10Gr, (b, e) 20Gr, (c, f) 30Gr.

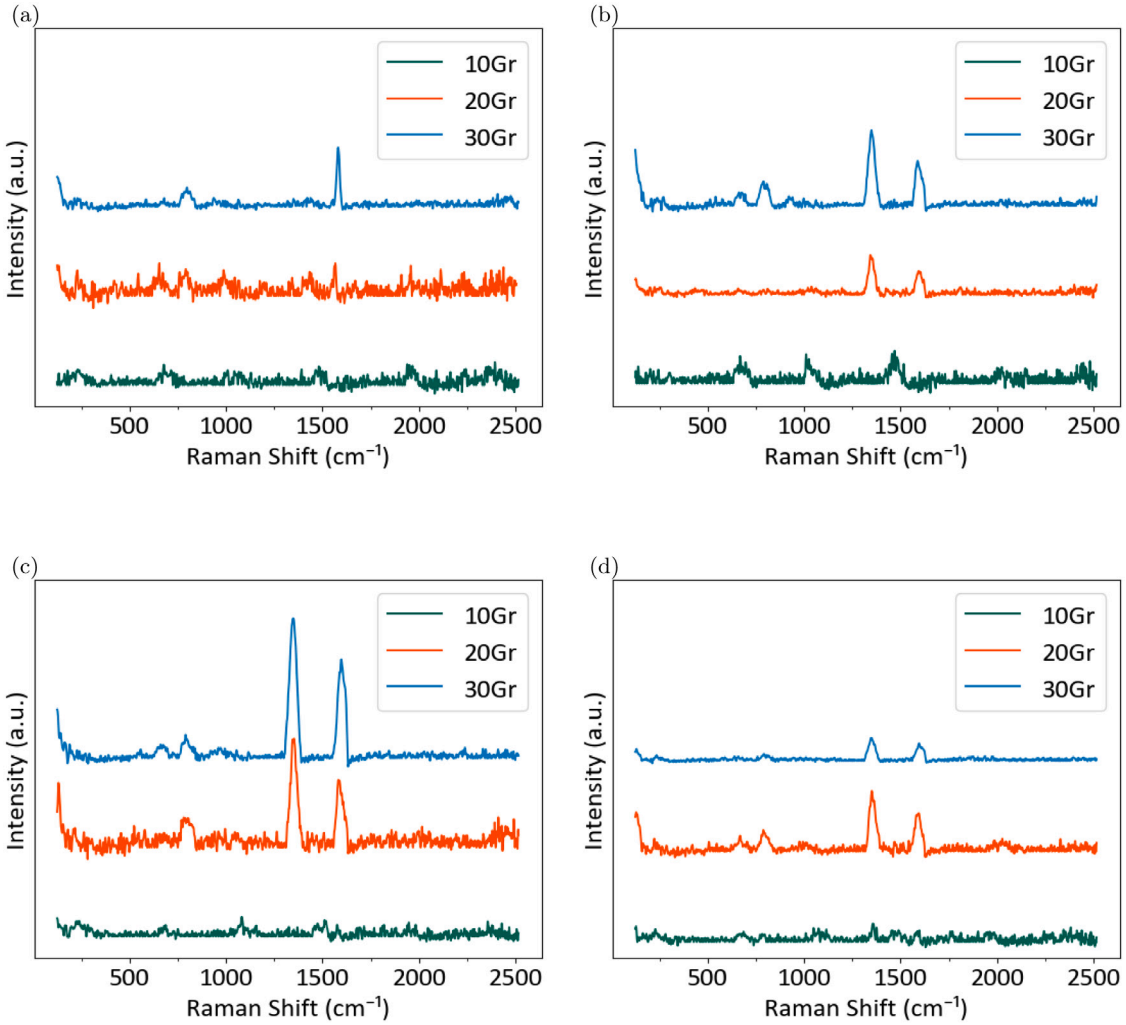

Fig. 9. Raman spectra of the different graphite–phenolic resin coatings at different stages of the tribological test. (a) unworn, (b) after 500 cycles, (c) after 1000 cycles, (d) after 10 000 cycles.

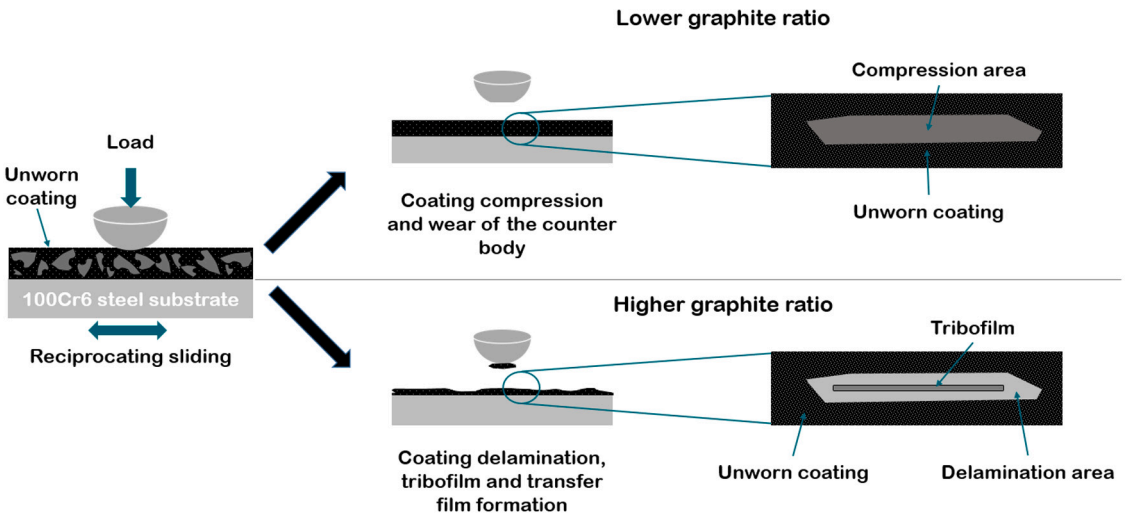

Fig. 10. Schematic representation of the hypothesized wear mechanism.

References

[1] E. Sliney, Solid Lubricants, NASA Cleveland, Ohio, 1991.
[2] T.W. Scharf, S.V. Prasad, Solid lubricants: a review, J. Mater. Sci. 48 (2) (2013) 511–531, [Online]. Available: http://link.springer.com/10.1007/s10853-012-7038-2.
[3] M. Alberts, K. Kalaitzidou, S. Melkote, An investigation of graphite nanoplatelets as lubricant in grinding, Int. J. Mach. Tools Manuf. 49 (12) (2009) 966–970, [Online]. Available: https://www.sciencedirect.com/science/article/pii/S0890695509001187.
[4] P.V. Muterlle, I. Cristofolini, M. Pilla, W. Pahl, A. Molinari, Surface durability and design criteria for graphite–bronze sintered composites in dry sliding applications, Mater. Des. 32 (7) (2011) 3756–3764, [Online]. Available: https://www.sciencedirect.com/science/article/pii/S0261306911002111.
[5] P. Li, W. He, P. Ju, L. Ji, X. Liu, F. Wu, Z. Lu, H. Li, L. Chen, J. Liu, H. Zhou, J. Chen, Acquisition of molecular rolling lubrication by self-curling of graphite nanosheet at cryogenic temperature, Nat. Commun. 15 (1) (2024) 5747, Publisher: Nature Publishing Group, [Online]. Available: https://www.nature.com/articles/s41467-024-49994-4.
[6] Y. Zhan, G. Zhang, Friction and wear behavior of copper matrix composites reinforced with SiC and graphite particles, Tribol. Lett. 17 (1) (2004) 91–98, [Online]. Available: https://doi.org/10.1023/B:TRIL.0000017423.70725.1c.
[7] W.H. Bragg, An Introduction to Crystal Analysis, G. Bell and Sons, Ltd., University Microfilms, London, Ann Arbor, 1928, OCLC, 287832.
[8] M. Dienwiebel, N. Pradeep, G.S. Verhoeven, H.W. Zandbergen, J.W. Frenken, Model experiments of superlubricity of graphite, Surf. Sci. 576 (1–3) (2005) 197–211, Publisher: Elsevier, [Online]. Available: https://www.sciencedirect.com/science/article/pii/S0039602804015584.
[9] A. Klemenz, A. Gola, M. Moseler, L. Pastewka, Contact mechanics of graphene-covered metal surfaces, Appl. Phys. Lett. 112 (6) (2018) 061601, [Online]. Available: https://doi.org/10.1063/1.5006770.
[10] M. Dienwiebel, G.S. Verhoeven, N. Pradeep, J.W.M. Frenken, J.A. Heimberg, H.W. Zandbergen, Superlubricity of graphite, Phys. Rev. Lett. 92 (12) (2004) 126101, [Online]. Available: https://link.aps.org/doi/10.1103/PhysRevLett.92.126101.
[11] C. Qu, K. Wang, J. Wang, Y. Gongyang, R.W. Carpick, M. Urbakh, Q. Zheng, Origin of friction in superlubric graphite contacts, Phys. Rev. Lett. 125 (12) (2020) 126102, Publisher: American Physical Society, [Online]. Available: https://link.aps.org/doi/10.1103/PhysRevLett.125.126102.
[12] A.P. Merkle, L.D. Marks, Friction in full view, Appl. Phys. Lett. 90 (6) (2007) 064101, [Online]. Available: https://doi.org/10.1063/1.2456192.
[13] R.H. Savage, Graphite lubrication, J. Appl. Phys. 19 (1) (1948) 1–10, [Online]. Available: https://doi.org/10.1063/1.1697867.
[14] D. Marchetto, T. Feser, M. Dienwiebel, Microscale study of frictional properties of graphene in ultra high vacuum, Friction 3 (2) (2015) 161–169, [Online]. Available: https://doi.org/10.1007/s40544-015-0080-8.
[15] C.E. Morstein, A. Klemenz, M. Dienwiebel, M. Moseler, Humidity-dependent lubrication of highly loaded contacts by graphite and a structural transition to turbostratic carbon, Nat. Commun. 13 (1) (2022) 5958, [Online]. Available: https://www.nature.com/articles/s41467-022-33481-9.
[16] K. Hasz, Z. Ye, A. Martini, R.W. Carpick, Experiments and simulations of the humidity dependence of friction between nanoasperities and graphite: The role of interfacial contact quality, Phys. Rev. Mater. 2 (12) (2018) 126001, Publisher: American Physical Society, [Online]. Available: https://link.aps.org/doi/10.1103/PhysRevMaterials.2.126001.
[17] D. Marchetto, P. Restuccia, A. Ballestrazzi, M.C. Righi, A. Rota, S. Valeri, Surface passivation by graphene in the lubrication of iron: A comparison with bronze, Carbon 116 (2017) 375–380, [Online]. Available: https://www.sciencedirect.com/science/article/pii/S000862231730129X.
[18] Q. Li, C. Lee, R.W. Carpick, J. Hone, Substrate effect on thickness-dependent friction on graphene, Phys. Status Solidi (B) 247 (11–12) (2010) 2909–2914, [Online]. Available: https://onlinelibrary.wiley.com/doi/abs/10.1002/pssb.201000555, _eprint: https://onlinelibrary.wiley.com/doi/pdf/10.1002/pssb.201000555.
[19] C. Morstein, M. Dienwiebel, Graphite lubrication mechanisms under high mechanical load, Wear 477 (2021) 203794, [Online]. Available: https://linkinghub.elsevier.com/retrieve/pii/S0043164821001836.
[20] A. Abe, J.A. Goss, M. Zou, Exploring the impact of spray process parameters on graphite coatings: morphology, thickness, and tribological properties, Coatings 14 (6) (2024) 714, Number: 6 Publisher: Multidisciplinary Digital Publishing Institute, [Online]. Available: https://www.mdpi.com/2079-6412/14/6/714.
[21] Y. Jia, H. Wan, L. Chen, H. Zhou, J. Chen, Effects of phosphate binder on the lubricity and wear resistance of graphite coating at elevated temperatures, Surf. Coat. Technol. 315 (2017) 490–497, [Online]. Available: https://linkinghub.elsevier.com/retrieve/pii/S0257897217302529.
[22] W. Huai, C. Zhang, S. Wen, Graphite-based solid lubricant for high-temperature lubrication, Friction 9 (6) (2021) 1660–1672, [Online]. Available: https://doi.org/10.1007/s40544-020-0456-2.
[23] P. Cai, T. Wang, Q. Wang, Effect of several solid lubricants on the mechanical and tribological properties of phenolic resin-based composites, Polym. Compos. 36 (12) (2015) 2203–2211, [Online]. Available: https://4spepublications.onlinelibrary.wiley.com/doi/10.1002/pc.23132.
[24] Q. Wang, X. Zhang, X. Pei, T. Wang, Friction and wear properties of solid lubricants filled/carbon fabric reinforced phenolic composites, J. Appl. Polym. Sci. 117 (4) (2010) 2480–2485, [Online]. Available: https://onlinelibrary.wiley.com/doi/10.1002/app.32154.
[25] F. Zhang, P. Yin, Q. Zeng, J. Wang, Insights on the formation mechanism of ultra-low friction of phenolic resin graphite at high temperature, Coatings 12 (1) (2022) 6, Number: 1 Publisher: Multidisciplinary Digital Publishing Institute, [Online]. Available: https://www.mdpi.com/2079-6412/12/1/6.
[26] E. Zhang, F. Gao, R. Fu, Y. Lu, X. Han, L. Su, Tribological behavior of phenolic resin-based friction composites filled with graphite, Materials 14 (4) (2021) 742, [Online]. Available: https://www.mdpi.com/1996-1944/14/4/742.
[27] K. Xu, Z. Yuan, Y. Luo, Y. Xie, Q. Xu, X. Gao, J. Xu, Frictional performance of surface-textured phenolic resin-impregnated graphite materials under water lubrication, Mater. Res. Express 10 (12) (2023) 125601, Publisher: IOP Publishing, [Online]. Available: https://doi.org/10.1088/2053-1591/ad125f.
[28] C. Zheng, X. Fang, H. Dou, W. Wang, K. Liu, J. Xu, Role of phenolic resin in the cryogenic tribological performance of impregnated graphite cooled by liquid nitrogen, Tribol. Int. 198 (2024) 109929, [Online]. Available: https://www.sciencedirect.com/science/article/pii/S0301679X24006819.
[29] A.C. Ferrari, Raman spectroscopy of graphene and graphite: Disorder, electron–phonon coupling, doping and nonadiabatic effects, Exploring graphene, Solid State Commun. 143 (1) (2007) 47–57, [Online]. Available: https://www.sciencedirect.com/science/article/pii/S0038109807002967.